Analysis of isospin dependence of nuclear collective flow in an isospin-dependent quantum molecular dynamics model

Chen Liewen,[1,2] Zhang Fengshou,[1,2,3] and Jin Genming[1,2]
[1]*Center of Theoretical Nuclear Physics, National Laboratory of Heavy Ion Accelerator, Lanzhou 730000, People's Republic of China*
[2]*Institute of Modern Physics, Academia Sinica, P.O. Box 31, Lanzhou 730000, People's Republic of China*
[3]*CCAST (World Laboratory), P.O. Box 8730, Beijing 100080, People's Republic of China*
(Received 24 April 1998)

Within the framework of an isospin-dependent quantum molecular dynamics model in which the initial neutron and proton densities are sampled according to the densities calculated from the Skyrme-Hartree-Fock method and the initial Fermi momenta of neutrons and protons are calculated from the Fermi gas model, we study systematically the transverse collective flow of different fragment types at an energy of 55 MeV/nucleon and the balance energy in the reactions ^{58}Fe+^{58}Fe and ^{58}Ni+^{58}Ni. The results from the present calculations indicate that the neutron-rich system (^{58}Fe+^{58}Fe) displays stronger negative deflection and has a higher balance energy, which are qualitatively in agreement with the experimental data. Furthermore, the effects of the isospin-dependent symmetry energy and nucleon-nucleon cross sections on collective flow are studied. [S0556-2813(98)07010-1]

PACS number(s): 25.70.Pq, 02.70.Ns, 24.10.Lx

I. INTRODUCTION

In recent years, with the establishment of secondary beam facilities at many laboratories around the world, radioactive beams of nuclei with large neutron or proton excess have been used, and heavy-ion physics has opened up a new field, radioactive nuclear beam (RNB) physics. Consequently, one can investigate the properties of nuclei very far from the β stability line and the isospin degree of freedom in nuclear reactions at wide energy ranges for different projectile-target combinations. Extensive reviews can be found in Refs. [1–4].

The isospin effects on preequilibrium nucleon emission [5–7] and isospin equilibrium and non-equilibrium in heavy-ion collisions (HIC) at intermediate energies [8,9] have been studied experimentally and theoretically. In particular, the isospin dependence of collective flow has become a very interesting subject of theoretical and experimental studies [10–12]. One knows that nuclear collective flow is a kind of collective phenomenon found in intermediate and high energy HIC, and the study of the dependence of collective flow on beam energy, mass number, and impact parameter, has revealed much interesting physics about the properties and origin of collective flow. Especially, from studying the beam energy dependence it has been found that the transverse collective flow in the reaction plane disappears at an incident energy which is called the balance energy $E_{\rm bal}$ [13–21]. Furthermore, detailed theoretical studies using microscopic transport models have shown that both the strength of transverse collective flow and the balance energy can be used to extract information about the nuclear equation of state (EOS) and in-medium nucleon-nucleon (N-N) cross sections [22–35]. Hence, studying collective flow in reactions induced by radioactive nuclei is very meaningful to explore the isospin-dependent part of the nuclear EOS and isospin-dependent N-N cross sections.

The isospin dependence of collective flow has been studied by Li *et al.* [10] in terms of an isospin-dependent Boltzmann-Uehling-Uhlenbeck (BUU) model in which the initial proton and neutron densities were calculated from the nonlinear relativistic mean-field (RMF) theory while the isospin dependence enters the model by using the experimental N-N cross sections and the isospin dependent nuclear mean field. The neutron-rich system was found to show stronger negative deflection at beam energies lower than $E_{\rm bal}$ and has a higher balance energy. Some predictions of the BUU model have been confirmed by experiments [11,12]. Although in Ref. [10] the isospin dependence of collective flow has been explained as competition among several mechanisms, such as N-N cross sections, symmetry energy, Coulomb energy, the surface properties of the colliding nuclei, and so on, the relative importance among these mechanisms is not yet clear. In particular, the BUU model cannot describe physically fragment flow since it is a one-body transport model and does not contain many-body correlation.

In order to investigate the isospin effects on collective flow and explain the recent experimental results, we have improved the original version of the QMD model [36–38] to include explicitly isospin degrees of freedom and get an isospin-dependent QMD (called IQMD hereafter) model, which includes isospin-dependent Coulomb potential, symmetry potential, N-N cross sections, and Pauli blocking. Moreover, in initialization of projectile and target nuclei, we sample separately neutrons and protons in phase space. Using the IQMD model, we study the fragment flow and its isospin effects in reactions ^{58}Fe+^{58}Fe and ^{58}Ni+^{58}Ni, which have the same mass number but different neutron/proton ratios. The calculated results indicate that the neutron-rich system (^{58}Fe+^{58}Fe) displays stronger negative transverse collective flow at energy of 55 MeV/nucleon and has a higher balance energy, which could be qualitatively in agreement with the experimental data. Meanwhile, the influence of the symmetry energy and N-N cross sections on the transverse collective flow has been also studied.

II. DESCRIPTION OF THE IQMD MODEL

The QMD model is classical in essence because the time evolution of the system is determined by classical canonical equation of motion, however, many important quantum features are included in this prescription. A comprehensive review can be found in Ref. [38]. In this paper, the main ideas in the IQMD model are introduced.

It is well known that the dynamics in HIC at intermediate energies is mainly governed by three components, namely, the mean field, two-body collisions, and Pauli blocking. Therefore, for an isospin-dependent reaction dynamics model it is essential that all three components should reasonably include isospin degrees of freedom. In addition, it is also important that, in initialization of projectile and target nuclei, the samples of neutrons and protons in phase space should be treated separately since there exists a large difference between neutron and proton density distributions for nuclei far from the β stability line. Particularly, for neutron-rich nucleus one should sample a stable initialized nucleus with neutron-skin structure and therefore one can directly explore the nuclear structure effects through a microscopic transport model. The IQMD model has been improved based on the above ideas. The following describes briefly IQMD model from four aspects, i.e., the mean field, two-body collisions, Pauli blocking, and initialization.

A. Mean field

In the IQMD model, the total interaction potential of the system is given by

$$U^{\mathrm{tot}}=U^{dd}+U^{\mathrm{Yuk}}+U^{\mathrm{Coul}}+U^{\mathrm{sym}}+U^{MDI} \tag{1}$$

with U^{dd} the density-dependent (Skyrme) potential, U^{Yuk} the Yukawa (surface) potential, U^{Coul} the Coulomb energy, U^{sym} the symmetry energy term, and U^{MDI} the momentum dependent interaction. The U^{dd} can be written as

$$U^{dd}=\alpha\left(\frac{\rho}{\rho_0}\right)+\beta\left(\frac{\rho}{\rho_0}\right)^{\gamma}, \tag{2}$$

with $\rho_0=0.16\,\mathrm{fm}^{-3}$.

For the momentum dependent interaction U^{MDI}, we make use of the real part of the optical potential parametrized in Ref. [39] as follows:

$$U^{MDI}=\delta\ln^2[\varepsilon(\mathbf{p_1}-\mathbf{p_2})^2+1]\frac{\rho}{\rho_0}. \tag{3}$$

The parameters of Eqs. (2) and (3) are given in Table I from which one can see two kinds of equations of state are commonly used. One is the so-called hard EOS (H, HM) with an incompressibility of $K=380\,\mathrm{MeV}$, and the other is the soft EOS (S, SM) with an incompressibility of $K=200\,\mathrm{MeV}$ [38]. The M refers to the inclusion of the momentum dependent interaction. The U^{Yuk}, U^{Coul}, and U^{sym} have the following forms [9]:

TABLE I. The parameter sets of Eqs. (2) and (3). The S and H refer to the soft and hard equation of state, the M refers to the inclusion of momentum dependent interaction, and the K refers to the incompressibility.

	K (MeV)	α (MeV)	β (MeV)	γ (MeV)	δ (MeV)	ε (c^2/GeV^2)
S	200	−356	303	1.17	–	–
SM	200	−390	320	1.14	1.57	500
H	380	−124	71	2.00	–	–
HM	380	−130	59	2.09	1.57	500

$$\begin{aligned}U^{\mathrm{Yuk}}=&\frac{1}{2}V_Y\sum_{i\neq j}\frac{1}{r_{ij}}\exp(Lm^2)\\&\times[\exp(-mr_{ij})\mathrm{erfc}(\sqrt{L}m-r_{ij}/\sqrt{4L})\\&-\exp(mr_{ij})\mathrm{erfc}(\sqrt{L}m+r_{ij}/\sqrt{4L}],\end{aligned} \tag{4}$$

$$U^{\mathrm{Coul}}=\frac{e^2}{4}\sum_{i\neq j}\frac{1}{r_{ij}}(1+t_{iz})(1+t_{jz})\mathrm{erf}(r_{ij}/\sqrt{4L}), \tag{5}$$

$$U^{\mathrm{sym}}=\frac{C}{2\rho_0}\sum_{i\neq j}t_{iz}t_{jz}\frac{1}{(4\pi L)^{3/2}}\exp\left[-\frac{(\mathbf{r}_i-\mathbf{r}_j)^2}{4L}\right], \tag{6}$$

with $V_Y=-0.0024\,\mathrm{GeV}$, $m=0.83$, and the L is the so-called Gaussian wave-packet width (here $L=2.0\,\mathrm{fm}^2$). The relative distance $r_{ij}=|\mathbf{r}_i-\mathbf{r}_j|$. The t_{iz} is the zth component of the isospin degree of freedom for the ith nucleon, which is equal to 1 and -1 for proton and neutron, respectively. The C is symmetry energy strength. From the above equations, one can see that the nuclear mean field is isospin dependent in the IQMD model.

B. Two-body collisions

In the IQMD model, two different parametrizations of N-N cross sections may be used optionally. One is the parametrization of Cugnon [40] (σ_{Cug}) which is isospin independent and the other is the experimental parametrization [41] (σ_{exp}) which is isospin dependent. It is shown that the neutron-proton cross section is about three times larger than the neutron-neutron or proton-proton cross section for the experimental parametrization at energies lower than 300 MeV/nucleon.

C. Pauli blocking

The method of considering the Pauli blocking effect is as follows. Whenever a collision has occurred, in the phase space we assume that each nucleon occupies a six-dimensional sphere with a volume of $h^3/2$ (considering the spin degree of freedom), and then calculate the phase volume, V, of the scattered nucleons being occupied by the rest nucleons with the same isospin as that of the scattered ones. We then compare $2V/h^3$ with a random number and decide whether the collision is blocked or not. Therefore, the Pauli blocking is isospin dependent, namely, the Pauli blocking of neutrons and protons is treated separately.

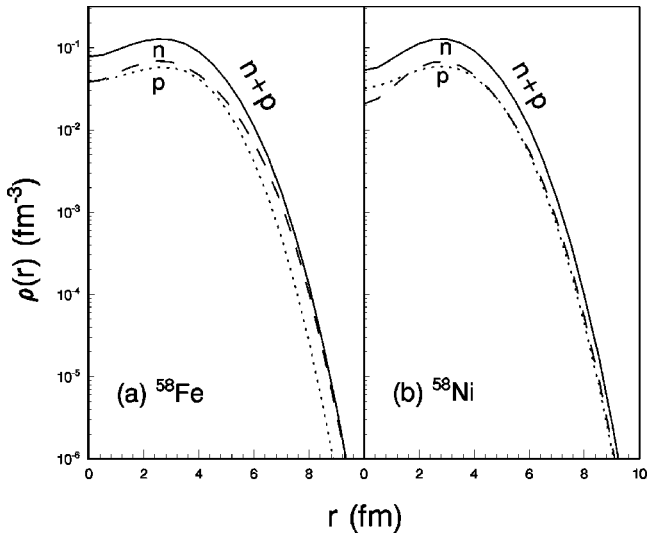

FIG. 1. Proton (dot), neutron (dash), and total (solid) density distributions in ^{58}Fe (a) and ^{58}Ni (b) calculated from Eq. (7).

D. Initialization

In the IQMD model, the neutron and proton are distinguished from each other in the initialization of projectile and target nuclei. The neutron and proton density distributions for the initial projectile and target nuclei are determined from the Skyrme-Hartree-Fock (SHF) method [42] with parameter set SKM* which can give reasonable density distribution for stable and neutron-rich nuclei [43]. Using the neutron and proton density distributions calculated from the SHF method, one can get the radial positions of neutrons and protons in the initial nuclei in terms of the Monte-Carlo method. In the QMD model, the radial density then can be written as

$$\rho(r)=\sum_i \frac{1}{(2\pi L)^{3/2}}\exp\left(-\frac{r^2+r_i^2}{2L}\right)\frac{L}{2rr_i} \times\left[\exp\left(\frac{rr_i}{L}\right)-\exp\left(-\frac{rr_i}{L}\right)\right]. \quad (7)$$

Figures 1(a) and (b) show the neutron, proton, and total density distributions sampled in initial nuclei, ^{58}Fe, and ^{58}Ni, respectively. We can see in Fig. 1 that there is a clear neutron skin in neutron-rich nucleus ^{58}Fe. While the total densities $(n+p)$ in ^{58}Fe and ^{58}Ni are almost identical, the total density in ^{58}Fe is more extended than that in ^{58}Ni. These features are in agreement with the results of the nonlinear RMF theory [10]. The momentum distribution of nucleons is generated by means of the local Fermi gas approximation. The local Fermi momentum $p_F^i(\mathbf{r})$ is given by

$$p_F^i(\mathbf{r})=\hbar(3\pi^2\rho_i(\mathbf{r}))^{1/3}, \quad (i=n,p). \quad (8)$$

The stability of the propagation of the initialized nuclei has been checked in detail and can last at least 200 fm/c according to the evolution of the average binding energies and root mean square radii of the initialized nuclei.

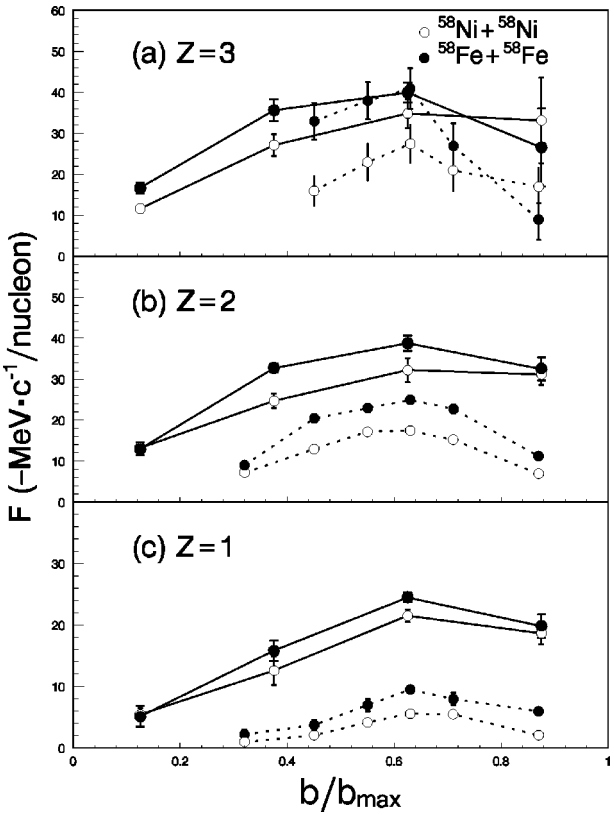

FIG. 2. Calculated (data connected by solid lines) and experimental (data connected by dotted lines) values of flow parameter as a function of the reduced impact parameter for three different fragment types, $Z=3$ (a), 2 (b), and 1 (c), from ^{58}Fe+^{58}Fe (solid circles) and ^{58}Ni+^{58}Ni (open circles) collisions at 55 MeV/nucleon.

III. RESULTS AND DISCUSSIONS

The important advantage of the QMD model is that it can explicitly represent the many body state of the system and thus contains correlation effects to all orders. Meanwhile, the QMD model treats statics and dynamics on an equal footing. Therefore, the QMD model provides important information about both the collision dynamics and the fragmentation process. Even though the BUU model is quite successful to describe one body observables, it fails in describing the formation of clusters. In this paper, we construct clusters in terms of the so-called coalescence model, in which particles with relative momenta smaller than P_0 and relative distances smaller than R_0 are considered to belong to one cluster. We adopted the parameter set $R_0=2.4$ fm and $P_0=200$ MeV/c following Refs. [44,45]. In addition, only the clusters with reasonable proton number Z and neutron number N, such as $Z=1$, $N=0$,1 and 2; $Z=2$, $N=1\sim6$; $Z=3$, $N=2\sim8$, are selected in order to get rid of nonphysical clusters.

A. Fragment flow

Using the IQMD model with parameter set SM, we calculate the flow parameters of different fragment types in reactions ^{58}Fe+^{58}Fe and ^{58}Ni+^{58}Ni at energy of 55 MeV/nucleon. The flow parameter is defined as the slope of the transverse momentum distribution at the center of the reduced center-of-mass (c.m.) rapidity $(y/y_{prog})_{c.m.}$. Figures 2(a), (b), and (c) give the calculated flow parameters of frag-

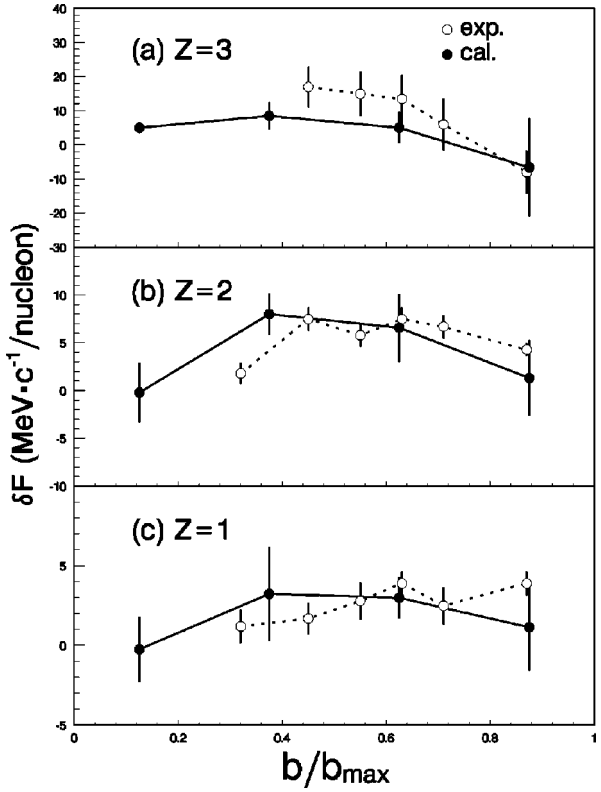

FIG. 3. Difference between the values of flow parameter for the data (open circles) and IQMD model predictions (solid circles) for ^{58}Ni+^{58}Ni and ^{58}Fe+^{58}Fe collisions at 55 MeV/nucleon versus reduced impact parameter for three different fragment types, $Z=3$ (a), 2 (b), and 1 (c). The lines are included only to guide the eye.

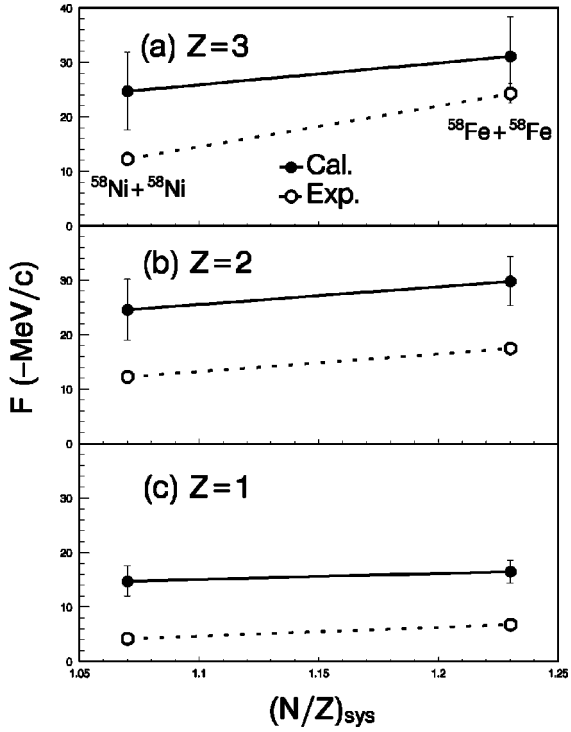

FIG. 4. Calculated (solid circles) and experimental (open circles) values of flow parameter as a function of the neutron/proton ratio of the reaction system for different fragment types, $Z=3$ (a), 2 (b), and 1 (c) from ^{58}Fe+^{58}Fe and ^{58}Ni+^{58}Ni at 55 MeV/nucleon. The lines are included only to guide the eye.

ments with $Z=3, 2$, and 1, respectively, as a function of the reduced impact parameter $b/b_{\max}$ (here $b_{\max}=8$ fm, the calculated values are connected by solid lines in Fig. 2). For each impact parameter, we perform a calculation of 500 events. In the present calculations, it is found that the multiplicity and transverse momenta for different fragment types have basically saturated by the end of 140 fm/c, therefore the calculated results actually correspond to the statistical average value of 3000 ''events'' which come from the sum of six time points from $t=150$ to 200 fm/c in each event. All the following calculations adopt this recipe. The errors shown are the statistical errors on the slopes of the linear fits. Meanwhile, the correspondent experimental values are also shown in Fig. 2 (the data points are connected by dotted lines in Fig. 2). The experimental values are extracted at the upper limit of each impact parameter bin [11]. It is shown in Fig. 2 that the calculated results are in agreement with the experimental data in trends. The difference in the magnitude of flow parameter between the two isotopic systems is maximal for semicentral collisions, which is qualitatively in agreement with the previous work [16,17]. In particular, the calculated results also show the isospin dependence of flow parameter for different fragment types, namely, the neutron-rich system (^{58}Fe+^{58}Fe) shows stronger negative deflection, which is in agreement with the predictions of the BUU model in Ref. [10] where the results are for all nucleons. Moreover, at large impact parameters for fragments with $Z=3$, we can see that both the calculated results and experimental data have a cross which may be because in the most peripheral collisions the number of N-N collisions is very small and the Coulomb interaction is more important so that the fragments with $Z=3$ have weaker Coulomb repulse in neutron-rich system. In addition, the mass dependence of the flow parameters shown in Fig. 2 also demonstrates the well-known increase in magnitude for heavier fragments [11,46–49]. This phenomenon may be because most nucleons are emitted by the hard stochastic collisions and hence the effect of the mean field is largely erased in the nucleon flow. This argument suggests that the flow of the composite fragment carries more direct information of the nuclear EOS than the nucleon flow.

From Fig. 2, it is seen that the predictions of the IQMD model systematically exhibit stronger values of flow parameter than the experimental data for all three fragment types at all reduced impact parameters. We shall give an explanation for this phenomenon in the following subsection. More importantly here, there is agreement between the data and the IQMD model predictions for the magnitude of the isospin effect, which is displayed in Fig. 3. The open (solid) circles are the difference between the values of flow parameter δF for the data (IQMD model predictions) in the isotopic systems ^{58}Ni+^{58}Ni and ^{58}Fe+^{58}Fe at each corresponding reduced impact parameter. The errors shown are statistical. It is shown that the isospin dependence predicted by the IQMD model is in agreement with the experimental data.

In order to see clearly the relation between flow parameter and neutron/proton ratios of the reaction system $(N/Z)_{\rm sys}$, we show in Figs. 4(a), (b), and (c) the impact-parameter-inclusive values of flow parameter for fragments with $Z=3, 2$, and 1, respectively, as a function of $(N/Z)_{\rm sys}$ of the

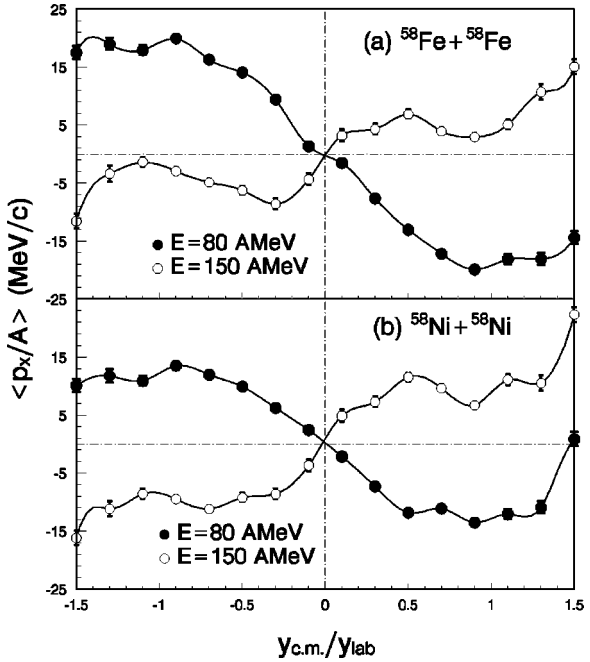

FIG. 5. Mean transverse momentum in the reaction plane versus the normalized rapidity for all nucleons from reactions ^{58}Fe+^{58}Fe (a) and ^{58}Ni+^{58}Ni (b) at two different incident energies, 80 MeV/nucleon (solid circles) and 150 MeV/nucleon (open circles). The curves are plotted to guide the eye.

systems ^{58}Fe+^{58}Fe (1.23) and ^{58}Ni+^{58}Ni (1.07). In the present calculations, we have simply assumed that the number of events is proportional to impact parameter b. Meanwhile, the experimental data are also shown in Fig. 4 (open circles). It is indicated that the calculated results are in good agreement with the experimental data in trends. From the above analyses we could conclude that the consideration of the isospin degree of freedom in the IQMD model is reasonable.

B. Disappearance of flow

From studying the beam energy dependence it has been found that the transverse collective flow changes from a negative one to a positive one at an incident energy, i.e., $E_{\rm bal}$, due to the competition between the attractive nuclear mean field potential and the repulsive N-N collisions [13–21]. The balance energy has been found to depend sensitively on the mass number, impact parameter, and properties of the colliding nuclei, such as the thickness of their surface [50]. Figures 5(a) and (b) show the distribution of transverse momentum versus the normalized rapidity $y_{\rm c.m.}/y_{\rm lab}$ for all nucleons at two different energies, 80 and 150 MeV/nucleon, with $b=3$ fm for the systems ^{58}Fe+^{58}Fe and ^{58}Ni+^{58}Ni, respectively. For both systems, at 80 MeV/nucleon the negative slopes (corresponding to negative scattering angles) are visible whereas at 150 MeV/nucleon the opposite sign slopes (positive scattering angles) are found. The former corresponds to negative flow parameter while the latter corresponds to the positive flow parameter.

The balance energy $E_{\rm bal}$ is obtained by a linear fit to the energy dependence of the flow parameter at the point where the flow parameter passes through zero. Figures 6(a), (b), (c), and (d) display the energy dependence of the flow parameter at $b=2$, 3, 4, and 5 fm, respectively, for systems ^{58}Fe+^{58}Fe (solid circles) and ^{58}Ni+^{58}Ni (open circles) with potential parameter set SM. It is shown that at different impact parameters the neutron-rich system (^{58}Fe+^{58}Fe) exhibits systematically smaller flow parameters, which implies a stronger attractive interaction in the reaction of the neutron-rich system. This feature is in agreement with the predictions of the BUU model [10]. From Fig. 4 in Ref. [10], one can see that the difference between flow parameters in ^{48}Cr+^{58}Ni and ^{48}Cr+^{58}Fe (neutron-rich system) decreases as the beam energy increases and finally disappears as the beam energy becomes far above the balance energy. However, this phenomenon is not observed in the present IQMD calculation at the small impact parameters, such as $b=2$, 3, and 4 fm. It is found in Figs. 6(a) and (b) that the difference between flow parameters in ^{58}Ni+^{58}Ni and ^{58}Fe+^{58}Fe (neutron-rich system) increases with increment of the beam energy. This phenomenon may be because with increment of the beam energy the N-N collisions become dominant and therefore the iso-

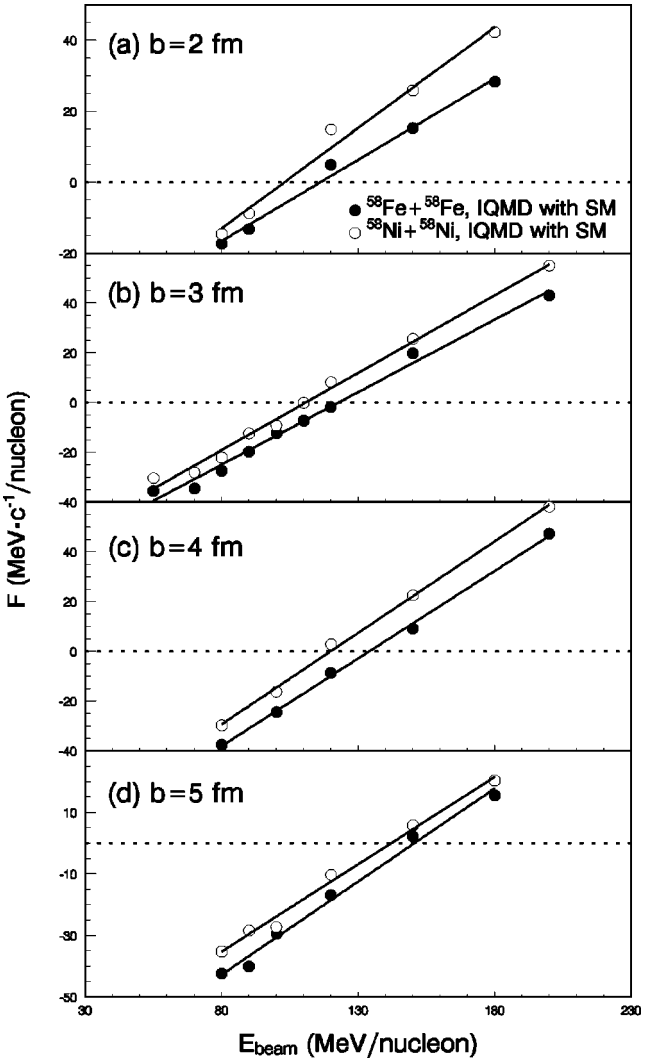

FIG. 6. Flow parameter for all nucleons as a function of incident energy at impact parameter $b=2$ (a), 3 (b), 4 (c), and 5 (d) fm for ^{58}Fe+^{58}Fe (solid circles) and ^{58}Ni+^{58}Ni (open circles). The straight lines are the results of linear fits.

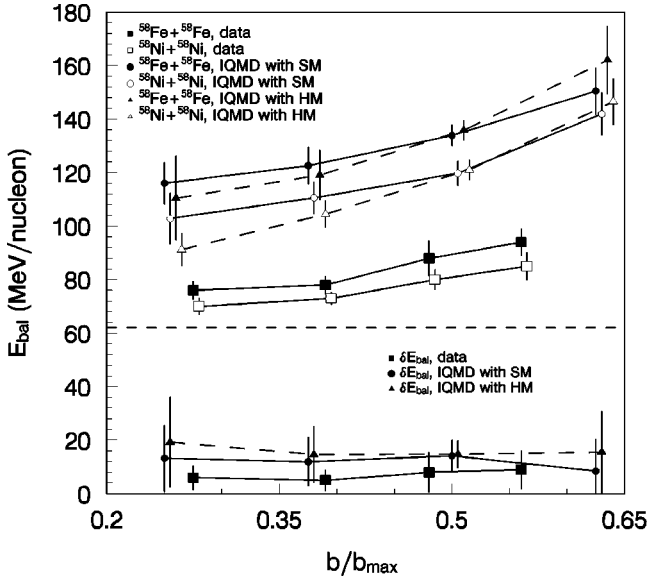

FIG. 7. (Upper window) Measured balance energies as a function of reduced impact parameter compared with the predictions of the IQMD model with potential parameter sets SM and HM. The solid (open) squares are measured for ^{58}Fe+^{58}Fe (^{58}Ni+^{58}Ni). The solid (open) circles are the predictions of the IQMD model with SM for ^{58}Fe+^{58}Fe (^{58}Ni+^{58}Ni) while the solid (open) triangles are the predictions of the IQMD model with HM for ^{58}Fe+^{58}Fe (^{58}Ni+^{58}Ni). (Lower window) The difference of the balance energies for the data (solid squares), predictions of the IQMD model with SM (solid circles), and predictions of the IQMD model with HM (solid triangles), in the isotopic systems ^{58}Ni+^{58}Ni and ^{58}Fe+^{58}Fe as a function of reduced impact parameter. The lines are included only to guide the eye.

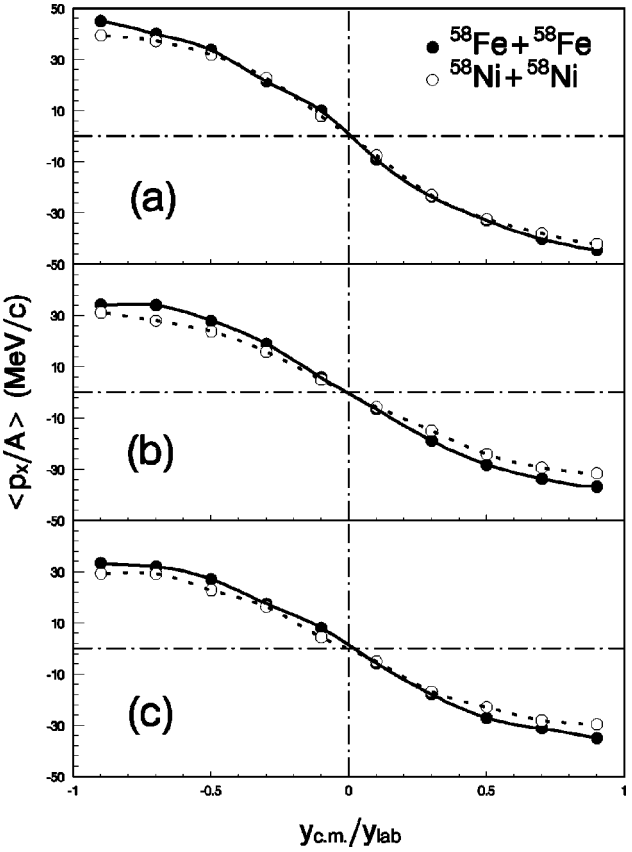

FIG. 8. Mean transverse momentum in the reaction plane versus the normalized rapidity for all nucleons from reactions ^{58}Fe+^{58}Fe (solid circles) and ^{58}Ni+^{58}Ni (open circles) at 55 MeV/nucleon and $b=5$ fm by using different C and parametrizations of N-N cross sections: $C=0$ with Cugnon's N-N cross sections σ_{Cug} (a), $C=0$ with experimental N-N cross sections σ_{exp} (b), and $C=32$ MeV with experimental N-N cross sections σ_{exp}. The curves are plotted to guide the eye.

spin dependence of the N-N cross sections plays a more important role. In fact, in the present calculations it is shown that the difference between the collision numbers per nucleon in ^{58}Ni+^{58}Ni and ^{58}Fe+^{58}Fe (neutron-rich system) increases as the beam energy increases. It should be mentioned that this phenomenon is complicated because it is related to many factors, such as the isospin-dependent N-N cross sections, the isospin-dependent Pauli blocking, beam energy, and so on. From Fig. 6 one can extract the balance energy at different impact parameters. The upper window in Fig. 7 displays the calculated E_{bal} with potential parameter sets SM and HM as a function of reduced impact parameter b/b_{max}; the experimental data from Ref. [12] are also included. The points, except for the predictions of the IQMD model with SM for ^{58}Fe+^{58}Fe and the experimental data for ^{58}Fe+^{58}Fe, have been offset in values of b/b_{max} for clarity. It is indicated that the values of E_{bal} predicted by the IQMD model with SM or HM are in agreement with the experimental data in trends. An approximate linear increase of the balance energy with impact parameter is visible in Fig. 7 (upper window), which is in agreement with the previous work [15,17]. It is also shown that the calculated values of E_{bal} with SM are roughly equal to those with HM, which implies that the balance energy is little dependent on incompressibility K and this is in agreement with the results of the BUU model calculations [21,51,52].

It is indicated in Fig. 7 (upper window) that the calculated values of E_{bal} with either SM or HM are systematically larger than the experimental data. However, from the lower set of points in Fig. 7 which display the difference of the balance energies δE_{bal} for the data (solid squares), predictions of the IQMD model with SM (solid circles), and predictions of the IQMD model with HM (solid triangles), respectively, between the isotopic systems ^{58}Ni+^{58}Ni and ^{58}Fe+^{58}Fe as a function of the reduced impact parameter, we can see that in error tolerance there is agreement between the data and the IQMD model predictions for the magnitude of the isospin effect. In the lower window of Fig. 7, the values for the predictions of the IQMD model with HM have been offset in the horizontal direction for clarity.

In fact, the previous calculated values of flow parameter for different fragment types are also systematically larger than the experimental data. The reason for these phenomena may be the low saturation densities in initial nuclei ^{58}Fe and ^{58}Ni. From Fig. 1 we can see both the saturation densities of ^{58}Fe and ^{58}Ni are about $0.12\,\mathrm{fm}^{-3}$ which is smaller than normal saturation density ρ_0, $0.16\,\mathrm{fm}^{-3}$, while the isospin-independent part of the nuclear EOS is attractive at low densities. As a matter of fact, Eq. (7) indicates that in the QMD

TABLE II. The flow parameters at different situations (see text) for ^{58}Fe+^{58}Fe and ^{58}Ni+^{58}Ni at beam energy of 55 MeV/nucleon and impact parameter $b=5$ fm.

Reaction systems	$C=0$ with $\sigma_{\rm Cug}$	$C=0$ with $\sigma_{\rm exp}$	$C=32$ MeV with $\sigma_{\rm exp}$
^{58}Fe+^{58}Fe	-34.8 ± 2.14 MeV	-29.1 ± 1.12 MeV	-27.9 ± 1.24 MeV
^{58}Ni+^{58}Ni	-33.8 ± 1.96 MeV	-24.5 ± 0.68 MeV	-24.1 ± 1.49 MeV

model the radial density is related to the Gaussian wave-packet width L. Even though the radial positions of the nucleons are reasonable, the radial density from Eq. (7) will result in some deviations from the real radial density. Moreover, the larger the L is, the larger the deviations are. Fortunately, this problem does not affect us to study the isospin effects on collective flow. Nevertheless, the previous calculated results are still in qualitative agreement with the experimental data. Particularly, the isospin dependence of the fragment flow and the balance energy is quantitatively in agreement with the experimental data.

C. Influence of symmetry energy and N-N cross sections on collective flow

Indeed, the isospin dependence of collective flow has been found in BUU model calculations and experiments and it has been explained as a result of the competition among several mechanisms in the reaction dynamics, such as N-N cross sections, symmetry energy, Coulomb energy, the surface properties of the colliding nuclei, and so on. However, the relative importance of these mechanisms is still not clear so far.

Using different symmetry energy strength C and parametrizations of N-N cross sections with potential parameter set SM, we show in Fig. 8 the distribution of average transverse momentum per nucleon for all nucleons versus the normalized rapidity $y_{\rm c.m.}/y_{\rm lab}$ for systems ^{58}Fe+^{58}Fe (solid circles) and ^{58}Ni+^{58}Ni (open circles) at energy of 55 MeV/nucleon and impact parameter $b=5$ fm. In Fig. 8(a) we use $C=0$ (no symmetry energy) and Cugnon's N-N cross sections $\sigma_{\rm Cug}$. The case of using $C=0$ and experimental N-N cross sections $\sigma_{\rm exp}$ is shown in Fig. 8(b). For the results shown in Fig. 8(c) we use $C=32$ MeV and experimental N-N cross sections $\sigma_{\rm exp}$. Figure 8 indicates that the neutron-rich system (^{58}Fe+^{58}Fe) exhibits stronger negative deflection for all of the above three cases. In order to give quantitative results, Table II shows the calculated values of flow parameter for the above three cases. The errors shown are statistical errors of the linear fits. From Table II one can see that both the $\sigma_{\rm exp}$ and symmetry energy make the strength of the flow parameter decrease, which implies that both N-N collisions and symmetry energy are repulsive as one expects [10]. Meanwhile, it is indicated that $\sigma_{\rm exp}$ has stronger influence in system ^{58}Fe+^{58}Fe than in system ^{58}Ni+^{58}Ni, which is easy to understand since N-N collisions result in repulsive flow and this effect is proportional to the number of collisions in the interaction volume. While the number of nucleons in this volume for the two reaction systems is roughly the same and the number of collisions in the reaction of the neutron-rich system is smaller since the neutron-neutron cross section is about a factor of three smaller than the neutron-proton cross section at energy of 55 MeV/nucleon. In addition, it is also shown that symmetry energy has stronger influence in system ^{58}Fe+^{58}Fe than in system ^{58}Ni+^{58}Ni, which results from the fact that in ^{58}Fe the difference between neutron and proton densities is larger and thus causes stronger symmetry energy. In the case of $C=0$ and $\sigma_{\rm Cug}$, the difference of the flow parameters of the two reactions may mainly come from the influence of the Coulomb potential and the surface properties of ^{58}Fe and ^{58}Ni. Unfortunately, we cannot study the influence of Coulomb potential on collective flow in this paper because we cannot get stable initial nuclei without Coulomb interaction.

IV. CONCLUSIONS

Based on an isospin-dependent QMD model in which the initial neutron and proton densities are sampled according to the densities calculated from the Skyrme-Hartree-Fock method and the initial Fermi momenta of neutron and proton are calculated from the Fermi gas model, we have sampled stable initial nuclei, ^{58}Fe and ^{58}Ni. The transverse collective flow of different fragment types and the balance energy in reactions ^{58}Fe+^{58}Fe and ^{58}Ni+^{58}Ni are studied systematically at different impact parameters. The results indicate that the neutron-rich system (^{58}Fe+^{58}Fe) displays stronger negative deflection and has a higher balance energy, which could be in qualitative agreement with the experimental data. In particular, the magnitude of the isospin effect could be quantitatively in agreement with the experimental data. Meanwhile, we also studied the influence of the isospin-dependent symmetry energy and N-N cross sections on collective flow.

From the analyses in this paper, we can conclude that the isospin dependence of collective flow is mainly determined by the isospin-dependent nuclear mean field and N-N cross sections. Moreover, it is also related to the surface properties of the colliding nuclei, beam energy, impact parameter, and so on. These results indicate that studying the isospin effects on collective flow is beneficial to exploring the isospin-dependent reaction dynamics.

ACKNOWLEDGMENTS

This work was supported by the National Natural Science Foundation of China under Grant No. 19600933, the Foundation of the Chinese Academy of Sciences, and the Foundation of National Educational Commission of the People's Republic of China.

[1] C. A. Bertulani, L. F. Canto, and M. S. Hussein, Phys. Rep. **226**, 281 (1993).
[2] M. V. Zukov, B. V. Danilin, D. V. Fedorov, J. M. Bang, I. J. Thompson, and J. S. Vaagen, Phys. Rep. **231**, 151 (1993).
[3] I. Tanihata, Prog. Part. Nucl. Phys. **35**, 505 (1995).
[4] B. A. Li, C. M. Ko, and W. Bauer, Int. J. Mod. Phys. E **7**, 147 (1998).
[5] L. W. Chen, X. D. Zhang, and L. X. Ge, High Energy Phys. Nucl. Phys. **20**, 1091 (1996); **21**, 486 (1997).
[6] G. J. Kunde, S. J. Gaff, C. K. Gelbke, T. Glasmacher, M. J. Huang, R. Lemmon, W. G. Lynch, L. Manduci, L. Matin, M. B. Tsang, W. A. Friedman, J. Dempsey, R. J. Charity, L. G. Sobotka, D. K. Agnihotri, B. Djerroud, W. U. Schroder, W. Skulski, J. Toke, and K. Wyrozebski, Phys. Rev. Lett. **77**, 2897 (1996).
[7] B. A. Li, C. M. Ko, and Z. Z. Ren, Phys. Rev. Lett. **78**, 1644 (1997).
[8] B. A. Li and S. J. Yennello, Phys. Rev. C **52**, 1746 (1995).
[9] L. W. Chen, L. X. Ge, X. D. Zhang, and F. S. Zhang, J. Phys. G **23**, 211 (1997).
[10] B. A. Li, Z. Z. Ren, C. M. Ko, and S. J. Yennello, Phys. Rev. Lett. **76**, 4492 (1996).
[11] R. Pak, W. Benenson, O. Bjarki, J. A. Brown, S. A. Hannuschke, R. A. Lacey, B. A. Li, A. Nadasen, E. Norbeck, P. Pogodin, R. E. Russ, M. Steiner, N. T. B. Stone, A. M. Vander Molen, G. D. Westfall, L. B. Yang, and S. J. Yennello, Phys. Rev. Lett. **78**, 1022 (1997).
[12] R. Pak, B. A. Li, W. Benenson, O. Bjarki, J. A. Brown, S. A. Hannuschke, R. A. Lacey, D. J. Magestro, A. Nadasen, E. Norbeck, R. E. Russ, M. Steiner, N. T. B. Stone, A. M. Vander Molen, G. D. Westfall, l. B. Yang, and S. J. Yennello, Phys. Rev. Lett. **78**, 1026 (1997).
[13] D. Krofcheck, W. Bauer, G. M. Grawley, C. Djalali, S. Howden, C. A. Ogilvie, A. M. Vander Molen, G. D. Westfall, W. K. Wilson, R. S. Tickle, and C. Gale, Phys. Rev. Lett. **63**, 2028 (1989).
[14] C. A. Ogilvie, D. A. Cebra, J. Clayton, P. Danielewicz, S. Howden, J. Karn, A. Nadasen, A. Vander Molen, G. D. Westfall, W. K. Wilson, and J. S. Winfield, Phys. Rev. C **40**, 2592 (1989).
[15] S. Soff, S. A. Bass, C. Hartnack, H. Stocker, and W. Greiner, Phys. Rev. C **51**, 3320 (1995).
[16] J. P. Sullivan, J. Peter, D. Cussol, G. Bizard, R. Brou, M. Louvel, J. P. Patry, R. Regimbart, J. C. Steckmeyer, B. Tamain, E. Crema, H. Doubre, K. Hagel, G. M. Jin, A. Peghaire, F. Saint-Laurent, Y. Cassagnou, R. Legrain, C. Lebrun, E. Rosato, R. MacGrath, S. C. Jeong, S. M. Lee, Y. Nagashima, T. Nakagawa, M. Ogihara, J. Kasagi, and T. Motobayasi, Phys. Lett. B **249**, 8 (1990).
[17] R. Pak, O. Bjarki, S. A. Hannuschke, R. A. Lacey, J. Lauret, W. J. Llope, A. Nadasen, N. T. B. Stone, A. M. Vander Molen, and G. D. Westfall, Phys. Rev. C **54**, 2457 (1996).
[18] W. M. Zhang, R. Madey, M. Elaasar, J. Schambach, D. Keane, B. D. Anderson, A. R. Baldwin, J. Cogar, J. W. Watson, G. D. Westfall, G. Krebs, and H. Wieman, Phys. Rev. C **42**, R491 (1990).
[19] D. Krofcheck, W. Bauer, G. M. Grawley, S. Howden, C. A. Ogilvie, A. Vander Molen, G. D. Westfall, W. K. Wilson, R. S. Tickle, C. Djalali, and C. Gale, Phys. Rev. C **46**, 1416 (1992).
[20] W. K. Wilson, W. Benenson, D. A. Cebra, J. Clayton, S. Howden, J. Karn, T. Li, C. A. Ogilvie, A. Vander Molen, G. D. Westfall, J. S. Winfield, B. Young, and A. Nadasen, Phys. Rev. C **41**, R1881 (1990).
[21] G. D. Westfall, W. Bauer, D. Craig, M. Cronqvist, E. Gualtieri, S. Hannuschke, D. Klakow, T. Li, T. Reposeure, A. M. Vander Molen, W. K. Wilson, J. S. Winfield, J. Yee, S. J. Yennello, R. Lacey, A. Elmaani, J. Lauret, A. Nadasen, and E. Norbeck, Phys. Rev. Lett. **71**, 1986 (1993).
[22] C. Gale, G. F. Bertsch, and S. Das Gupta, Phys. Rev. C **35**, 1666 (1987).
[23] J. Zhang, S. Das Gupta, and C. Gale, Phys. Rev. C **50**, 1617 (1994).
[24] M. B. Tsang, G. F. Bertsch, W. G. Lynch, and M. Tohyama, Phys. Rev. C **40**, 1685 (1989).
[25] H. M. Xu, Phys. Rev. Lett. **67**, 2769 (1991).
[26] B. A. Li, Phys. Rev. C **48**, 2415 (1993).
[27] P. Danielewicz and G. Odyniec, Phys. Lett. **157B**, 146 (1985).
[28] J. J. Molitoris and H. Stocker, Phys. Lett. **162B**, 47 (1985).
[29] J. J. Molitoris, D. Hahn, and H. Stocker, Nucl. Phys. **A447**, 13c (1986).
[30] G. F. Bertsch, W. G. Lynch, and M. B. Tsang, Phys. Lett. B **189**, 384 (1987).
[31] P. Danielewicz, H. Strobele, G. Odyniec, D. Bangert, R. Bock, R. Brockmann, J. W. Harris, H. G. Pugh, W. Rauch, R. E. Renfordt, A. Sandoval, D. Schall, L. S. Schroeder, and R. Stock, Phys. Rev. C **38**, 120 (1988).
[32] V. de la Mota, F. Sebille, M. Farine, B. Remaud, and P. Schuck, Phys. Rev. C **46**, 677 (1992).
[33] Q. Pan and P. Danielewicz, Phys. Rev. Lett. **70**, 2062 (1993).
[34] H. B. Zhou, Z. X. Li, Y. Z. Zhuo, and G. J. Mao, Nucl. Phys. **A580**, 627 (1994).
[35] G. J. Mao, Z. X. Li, Y. Z. Zhuo, and Z. Q. Yu, Phys. Lett. B **327**, 183 (1994).
[36] C. Hartnack, Z. X. Li, L. Neise, G. Peilert, A. Rosenhauer, H. Sorge, J. Aichelin, H. Stocker, and W. Greiner, Nucl. Phys. **A495**, 303c (1989).
[37] Q. L. Zhu, L. X. Ge, and X. D. Zhang, High Energy Phys. Nucl. Phys. **16**, 658 (1992).
[38] J. Aichelin, Phys. Rep. **202**, 233 (1991).
[39] J. Aichelin, A. Rosenhauer, G. Peilert, H. Stocker, and W. Greiner, Phys. Rev. Lett. **58**, 1926 (1987).
[40] J. Cugnon, T. Mizutani, and J. Vandermeulen, Nucl. Phys. **A352**, 505 (1981).
[41] K. Chen, Z. Fraenkel, G. Friedlander, J. R. Grover, J. M. Miller, and Y. Shimamoto, Phys. Rev. **166**, 949 (1968).
[42] P. G. Reinhard, in *Computational Nuclear Physics 1,* edited by K. Langanke, J. A. Maruhn, and S. E. Koonin (Springer-Verlag, Germany, 1991), pp. 28–50.
[43] W. X. Wen, G. M. Jin, and J. Q. Zhong, High Energy Phys. Nucl. Phys. **20**, 148 (1996).
[44] F. S. Zhang and E. Suraud, Phys. Rev. C **51**, 3201 (1995).
[45] H. Kruse, B. V. Jacak, J. J. Molitoris, G. D. Westfall, and H. Stocker, Phys. Rev. C **31**, 1770 (1985).
[46] D. R. Bowman, G. F. Peaslee, R. T. de Souza, N. Carlin, N. K. Gelbke, W. G. Gong, Y. D. Kim, M. A. Lisa, W. G. Lynch, L. Phair, M. B. Tsang, C. Williams, N. Colonna, K. Hanold, M. A. McMahan, G. J. Wozniak, L. G. Moretto, and W. A. Friedman, Phys. Rev. Lett. **67**, 1527 (1991).
[47] J. Hubele, P. Kreutz, J. C. Adloff, M. Begemann-Blaich, P. Bouissou, G. Imme, I. Iori, G. J. Kunde, S. Leray, V. Lindenstruth, Z. Liu, U. Lynen, R. J. Meijer, U. Milkau, A. Moroni,

W. F. J. Muller, C. Ngo, C. A. Ogilvie, J. Pochodzalla, G. Raciti, G. Rudolf, H. Sann, A. Schuttauf, W. Seidel, L. Stuttge, W. Trautmann, and A. Tucholski, Z. Phys. A **340**, 263 (1991).

[48] J. Peter, in *International Symposium on Heavy Ion Physics and its Applications*, Lanzhou, China (World Scientific, Singapore, 1990), p. 191.

[49] L. W. Chen, F. S. Zhang, and X. H. Zeng, High Energy Phys. Nucl. Phys. **22**, 538 (1998).

[50] D. Klakow, G. Welke, and W. Bauer, Phys. Rev. C **48**, 1982 (1993).

[51] W. Bauer, Phys. Rev. Lett. **61**, 2534 (1988).

[52] W. Bauer, C. K. Gelbke, and S. Pratt, Annu. Rev. Nucl. Part. Sci. **42**, 77 (1992).